Microscopic dynamics in liquid lithium

A. Torcini,[1,2] U. Balucani,[1] P. H. K. de Jong,[3] and P. Verkerk[3]
[1]*Istituto di Elettronica Quantistica, Consiglio Nazionale delle Ricerche, 50127 Firenze, Italy*
[2]*Dipartimento di Fisica dell'Università e Istituto Nazionale di Fisica della Materia, 50125 Firenze, Italy*
[3]*Interfacultair Reactor Instituut, Technische Universiteit Delft, 2629 JB Delft, The Netherlands*
(Received 15 August 1994)

A detailed analysis of the dynamic properties of liquid lithium at three distinct thermodynamic points has been performed by computer simulation. The reliability of the adopted potential model is supported by a comparison with neutron- and x-ray scattering data. Several dynamical properties (both single-particle and collective) are subsequently investigated, and their evolution with temperature compared with the one reported in recent experiments. On the theoretical side, it is particularly interesting to focus on single-particle features. We show that most of them (including ordinary and space-dependent diffusion) can satisfactorily be interpreted by a simplified mode-coupling approach.

PACS number(s): 61.20.Ja, 61.25.Mv

I. INTRODUCTION

Together with rare-gas fluids, molten alkali metals have always been considered as paradigms of the behavior shown by the so-called "simple liquids" [1]. In the last few years, the appearance of new accurate data for the time-dependent properties of these systems has led to a renewed interest and to the possibility of more stringent tests for our understanding of the dynamics of the liquid state. On the experimental side, neutron-scattering experiments have, in fact, been performed in liquid caesium [2], liquid sodium [3,4], and liquid lithium [5,6]. As far as liquid lithium is concerned, a recent investigation by inelastic x-ray scattering is also available [7]. A natural consequence of all this activity has been the appearance of several simulation [8–10] and theoretical [11–17] studies, mostly devoted to temperatures T near the melting point T_m.

In this work, we investigate the dynamical features of liquid lithium at three different thermodynamic points, which correspond to those explored in the neutron-scattering experiments quoted in [5]. As we shall see later on (see also Refs. [5] and [18]), for liquid lithium the extraction of the relevant pieces of information from the experimental data is not straightforward. Consequently, for this element both simulation and theoretical investigations are expected to be extremely useful. Up to now, only a limited number of simulation studies concerning the dynamic properties have been published [10,15].

A preliminary examination of this liquid reveals that above $T_m = 453$ K, lithium can be considered as an essentially classical system. On the structural point of view, the thermal wavelength $\Lambda = (2\pi\hbar^2/mk_BT)^{1/2}$ (m being the atomic mass) turns, in fact, to be considerably less than the average interatomic distance $a = (1/n)^{1/3}$, where n is the number density. In particular, at $T = T_m$, one finds that $\Lambda/a = 0.11$. As far as dynamics is concerned, the frequency range for which the liquid can be regarded as classical can be estimated by demanding that the detailed balance factor $\exp(-\hbar\omega/2k_BT)$ is ≈ 1. At the melting point, this criterion turns out to be satisfied up to $\omega \approx 120$ ps^{-1}; the frequencies considered in the present investigation are always considerably smaller than this upper limit. These circumstances make the study of liquid lithium feasible by classical computer simulation experiments.

From a purely theoretical point of view, one can take advantage of the progress achieved in the 1980s in the development of nonphenomenological approaches for liquid-state dynamics [19]. An important result in this respect has been the recognition [20,21] of two different kinds of processes ruling the decay of the relevant time correlations, namely a fast decay channel determined by "binary" collisional events, and an additional long-lasting mechanism, associated with correlated collisions and due to the couplings of the dynamical variable of interest with the slow "modes" present in the fluid (the so-called *mode-coupling* decay channels). A simplified version of these theories has recently been developed, with quite satisfactory results for the leading transport properties (diffusion and shear viscosity coefficients) as well as for several aspects of the single-particle dynamics near the melting point [11–14].

The paper is organized as follows. The next two sections concern a short technical review of the neutron-scattering experiments reported in detail in Ref. [5] (Sec. II), as well as a discussion of the corresponding computer simulations as implemented in the present work (Sec. III). In addition, in Sec. III we shall compare the results obtained by various techniques for the structural properties of liquid lithium at several temperatures. Section IV is devoted to the collective dynamics of the system, and to a comparison between the neutron-scattering data and our simulation findings. Single-particle dynamical properties (in particular, the velocity autocorrelation function and the self-intermediate scattering function) are discussed in Sec. V in terms of a memory function framework. Finally, Sec. VI summarizes the main results of the work, along with a few concluding remarks.

II. NEUTRON-SCATTERING MEASUREMENTS

Microscopic dynamic processes (ranging, e.g., from mass diffusion to short-wavelength sound propagation) occur in liquid lithium over rather different time scales. In a study of these features by neutron-scattering experiments, it is necessary to vary considerably the incident neutron energy in view of the limited relative resolution in energy. The experimental data discussed in this paper were consequently obtained by two distinct sets of experiments with different energy resolutions. Specifically, two time-of-flight spectrometers have been used: RKS at the 2 MW reactor in Delft, and MARI at the neutron spallation source ISIS in England. The incident neutron wavelength in the RKS experiment was 2.00 Å (corresponding to an energy of 20.5 meV), with an energy resolution of 1.4–1.6 meV (or 2.0–2.4 ps^{-1} in terms of frequency). On MARI, we used 0.39-Å neutrons (incident energy 525 meV), with a resolution of 15 meV (23 ps^{-1}).

Since natural lithium contains ^{6}Li, which is a strong neutron absorber, in both experiments the samples consisted of highly enriched ^{7}Li. Neutron scattering from this isotope may be coherent as well as incoherent, with a nearly equal probability (see Sec. IV). As a result, the measured time-of-flight spectra are proportional to a weighted sum of the dynamic structure factor $S(k,\omega)$ and of its self-part $S_s(k,\omega)$.

For values of the wave vector k smaller than the position k_m of the main peak of the static structure factor $S(k)$, the shapes of the two dynamic structure factors as a function of ω (and, in particular, the spectral widths) differ considerably. In this k region, the RKS data with 20.5-meV neutrons mainly provides information on the relatively narrow self-spectrum $S_s(k,\omega)$. On the other hand, due to the high sound velocity in liquid lithium ($\approx$4500 m/s near T_m), information on collective phenomena can only be provided by the MARI experiment, which uses incident neutrons of relatively high energy (525 meV). The separation of the two contributions is made easier by the large qualitative differences between $S(k,\omega)$ and $S_s(k,\omega)$ [5].

TABLE I. The states of liquid lithium investigated in our simulations (the number densities n and the temperatures T are the same as those of the neutron-scattering experiments of Ref. [5]). The corresponding parameters ε and σ of the PST effective potential $v(r)$ [21] are also reported [ε is the depth of the main potential well and σ the position of the first zero of $v(r)$]. The quantity $\tau_0=(m\sigma^2/\varepsilon)^{1/2}$ establishes a basic time unit for the dynamics.

Parameter \ T (K)	470	526	574
n (Å^{-3})	0.0445	0.0441	0.0438
σ (Å)	2.6839	2.6837	2.6835
ε (K)	581.63	584.54	586.76
τ (ps)	0.3215	0.3225	0.3218

The situation changes as the wave vector k approaches k_m. Here the presence of "de Gennes narrowing" [22] makes the width of $S(k,\omega)$ comparable with the one of $S_s(k,\omega)$; as a consequence, the resolution of the MARI experiment becomes insufficient, and the relevant information can only be provided by the RKS data.

Whereas the RKS experiment was performed at the three thermodynamic states reported in Table I, the MARI data concern only the state at $T=470$ K (namely, the one closest to the melting point). We refer the reader to [5] for a full detail of the two experiments.

III. MOLECULAR DYNAMICS SIMULATIONS AND THE STRUCTURAL PROPERTIES

The molecular dynamics (MD) simulations have been performed within the usual microcanonical ensemble, at three state points which closely correspond to those of the neutron experiments (see Table I). More specifically, after an equilibration time of 80–100 ps the equations of motion of $N=250$ "lithium" particles, enclosed in a cubic box with periodic boundary conditions, have been integrated up to 240 ps by a Verlet algorithm with a time step $\delta t=2$ fs. To make a closer contact with the experiment, we have considered particles of mass $m=11.65\times10^{-24}$ g, corresponding to that of the isotope ^{7}Li. A rough measure of the overall accuracy of the integration is provided by the variations of the total energy, which are of the order of 4–5 parts in 10^4.

The adopted interionic potential $v(r)$ is the well known effective potential implemented by Price, Singwi, and Tosi (PST) [23] to reproduce at an atomic level the main features of alkali metals in the solid phase. The PST potential has successfully been used to account for the basic structural and dynamical properties of liquid Na, K, Rb, and Cs [14,17,24,25]. In particular, Balucani, Torcini, and Vallauri [14] have shown that the PST potentials for Na, K, Rb, and Cs at their respective melting points nearly coincide when plotted in terms of the length σ [the position of the first zero of $v(r)$] and of the energy ε [the value of the main minimum of $v(r)$]. In this case, the reduced density $n^*=n\sigma^3$ is about the same for all these alkalis ($n^*\approx0.895$), and their reduced temperatures $T^*=k_BT/\varepsilon$ lie in the interval 0.78–0.84. As a result, a common behavior is expected (and indeed observed [14]) even for the static and dynamic correlation functions. Liquid lithium at $T=470$ K (in proximity of its melting point) has also a $T^*\approx0.80$ in the above range; however, its reduced density $n^*=0.860$ differs by 4% from those of the other alkalis. Although the reduced PST potential $v(r)/\varepsilon$ still nearly coincides with those pertinent to the other alkalis (see Fig. 1), the small difference in the reduced density has the effect of leading to a worse scaling behavior of the measured static and dynamical properties when compared with the other elements. This reflects the fact that for a simple liquid near the melting point, the role of density is more important than that of temperature. Figure 1 illustrates the PST potential for Li at 470 K; the reduced potentials at the other two state points of interest do not differ appreciably from the one reported in this figure.

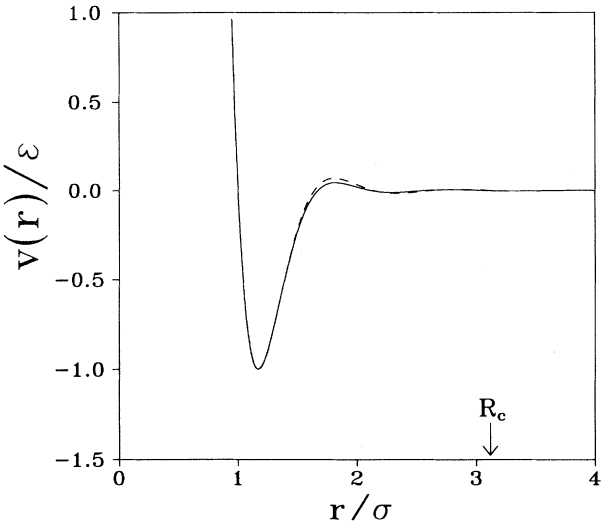

FIG. 1. The PST potential for liquid lithium at $T=470$ K and $n=0.0445$ Å^{-3} (full line). R_c denotes the cutoff radius adopted in our simulations. For the sake of comparison, the PST potential appropriate to liquid caesium at 380 K is also reported (dashed line).

The static structure factors $S(k)$ as deduced from neutron and x-ray diffraction at the three considered temperatures are compared in Fig. 2 with those obtained in our simulations. Despite a good overall agreement among these data, some discrepancies are apparent. These are partly due to the fact that in lithium both the neutron and x-ray data are affected by uncertainties larger than those in the other alkali metals [18]. Also, it is well known that the two experimental techniques may give slightly different results, particularly at small k. A closer look at these differences reveals the situation illustrated in Fig. 3, which refers to $T=470$ K and $k \leq 1.6$ Å^{-1}. It is apparent that while the simulation results compare rather well with the x-ray data reported in Ref. [18], the comparison with the neutron results is less favorable. Note that the MD results of $S(k)$ as $k \rightarrow 0$ have been obtained by extrapolating the values of $S(k)$ at finite wave vectors in terms of a quadratic law. The values of $S(0)$ deduced in this way are found to be in good agreement with those calculated from the isothermal compressibility data reported in [26]: in particular, they reproduce the increase of $S(0)$ observed at the higher temperatures (see Table II).

TABLE II. The small wave vector limit of the static structure factor $S(k)$, as obtained from our MD data and from the compressibility data of Ref. [26].

Static structure factor \ T (K)	470	526	574
$S_{MD}(0)$	0.029	0.035	0.039
$S_{expt}(0)$	0.027	0.033	0.037

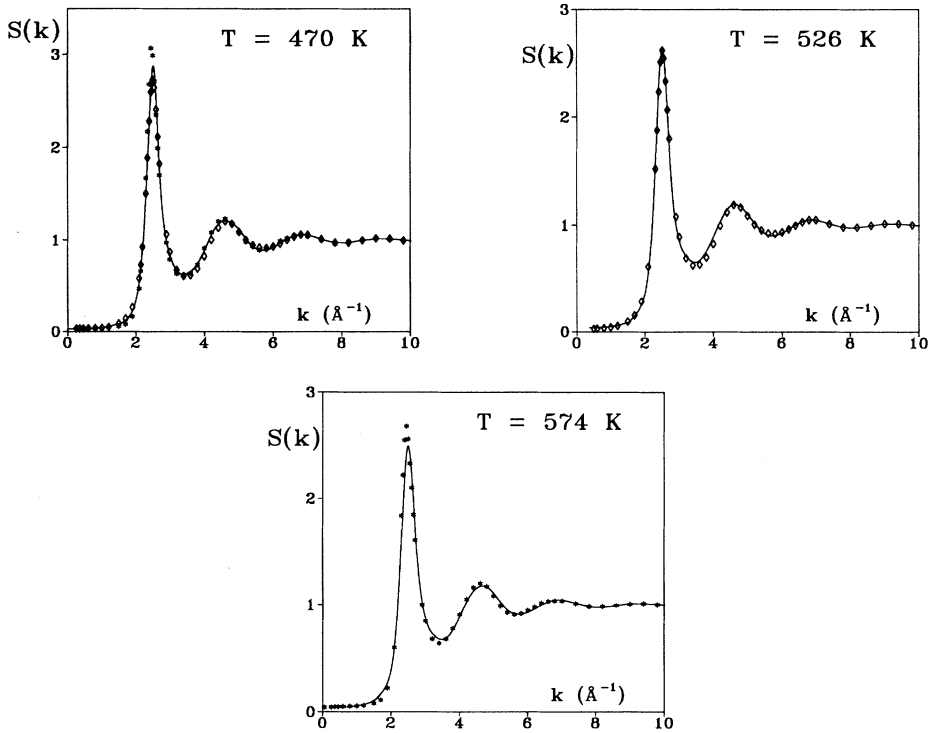

FIG. 2. Static structure factors for liquid Li at the three state points reported in Table I. The solid line refers to our molecular dynamics (MD) results, while the asterisks and the lozenges denote the diffraction data obtained by neutrons and by x rays, respectively (both taken from Ref. [19]).

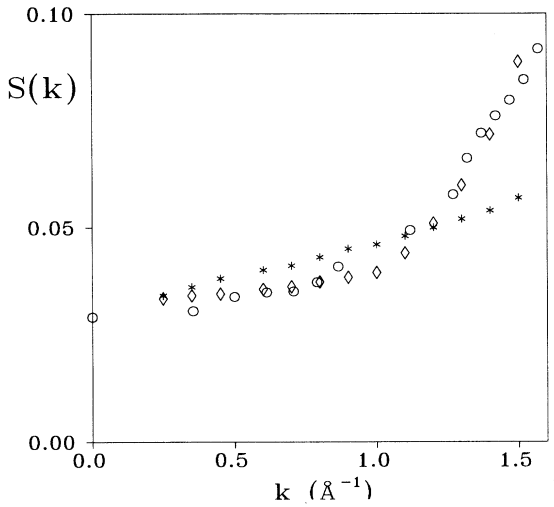

FIG. 3. Small k behavior of $S(k)$, as obtained by our MD data (circles), by neutron diffraction (asterisks), and by x-ray diffraction (lozenges).

IV. COLLECTIVE DYNAMICS

As already mentioned, the dynamical properties of liquid lithium have recently been investigated by inelastic neutron scattering (INS) at the three temperatures $T=470$, 526, and 574 K [5] and by inelastic x-ray scattering (IXS) at $T=533$ K [7]. Since IXS is purely coherent, the x-ray data probe only properties associated with the collective dynamics of the system, namely those described by the dynamic structure factor $S(k,\omega)$. In contrast, by INS one is able (at least in principle) to obtain information on both the self and the collective motions of the particles. However, in the specific case of interest the mixed-scatterer nature of lithium poses difficult problems for the extraction of the self and the collective contributions to the total dynamic structure factor

$$S_{\mathrm{tot}}(k,\omega)=\frac{1}{\sigma_i+\sigma_c}[\sigma_i S_s(k,\omega)+\sigma_c S(k,\omega)] \tag{1}$$

as obtained from the experiment. In Eq. (1) σ_i and σ_c denote, respectively, the incoherent and coherent scattering cross sections, which turn out to be remarkably similar in ^{7}Li ($\sigma_i=0.68$ and $\sigma_c=0.62$ b). Hence, if from $S_{\mathrm{tot}}(k,\omega)$ one wishes to deduce separate data for $S_s(k,\omega)$ and $S(k,\omega)$ it is, in general, necessary to resort to some phenomenological model, suitably adapted in such a way to fit the experimental data [5]. In this situation, properly designed MD simulations are extremely useful because they allow a direct insight into quantities not easily accessible by experiment.

From the above, it is clear that a direct comparison of the MD results with INS data can be made only at the level of $S_{\mathrm{tot}}(k,\omega)$. Such a comparison at selected wave vectors is reported in Figs. 4 and 5 for the three considered temperatures. The overall agreement is seen to be

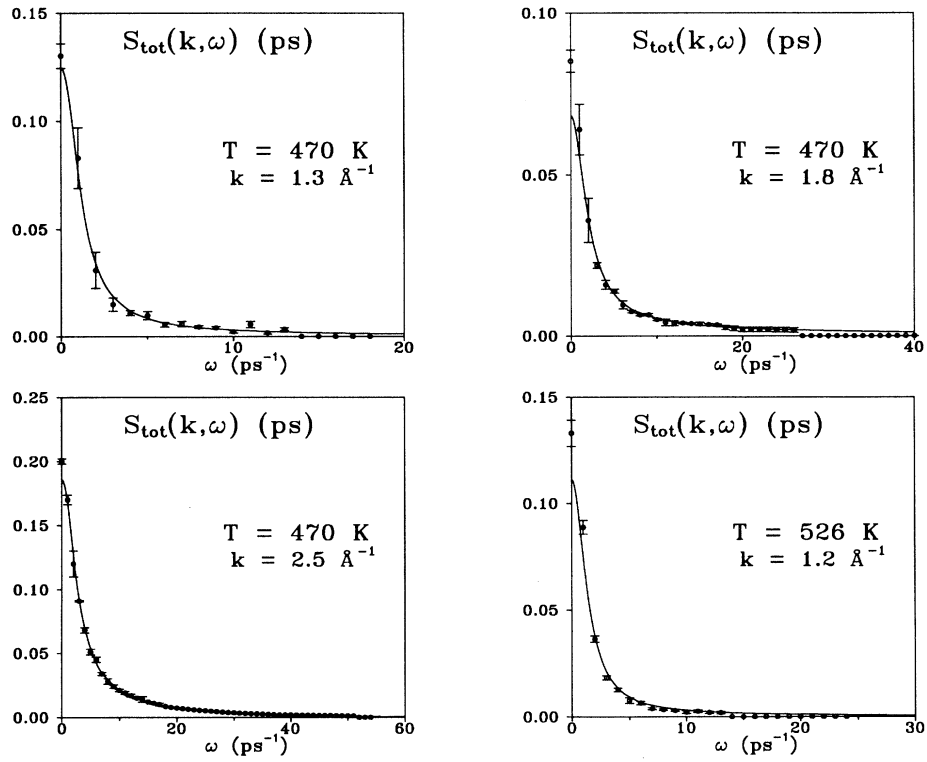

FIG. 4. Temperature dependence of the total dynamic structure factor of liquid Li at several wave vectors. Full line, our MD findings: circles, neutron-scattering results [2].

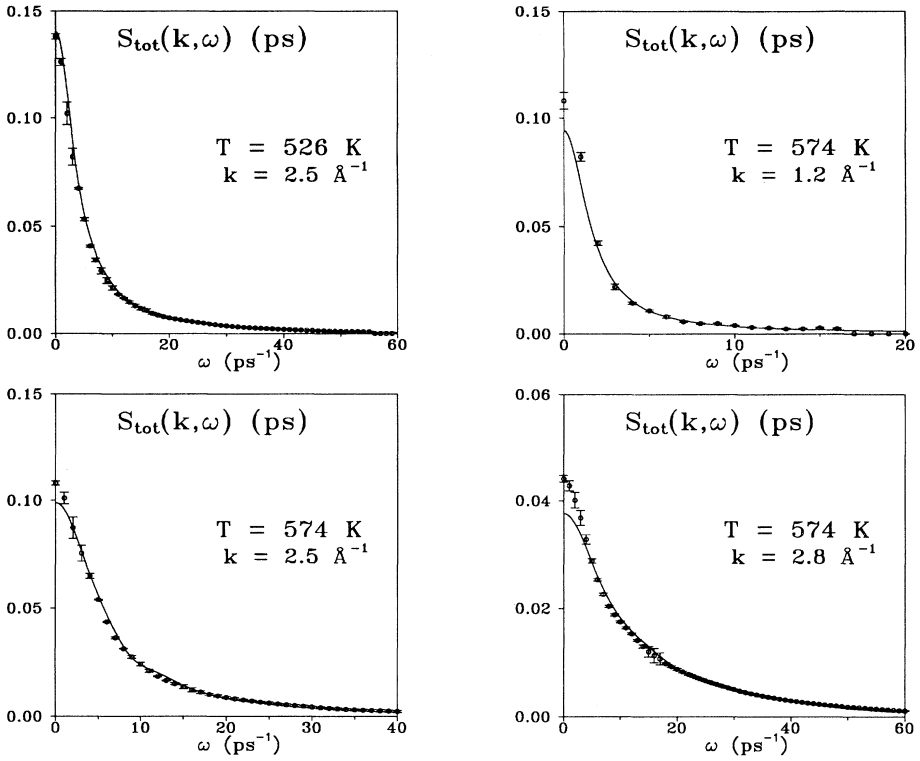

FIG. 5. As in the previous figure.

quite satisfactory, except for the amplitudes of the quasielastic peak at $\omega \approx 0$. These discrepancies are not connected to the choice of the PST potential: Similar MD results for lithium at 470 K have recently been obtained by adopting a different $v(r)$ [10]. Even so, the possibility of some inadequacy of the potentials proposed up to now to simulate liquid lithium [15,23] cannot be ruled out *a priori*. A detailed analysis [15] of several pseudopotentials (both local and nonlocal) introduced to account for the interaction among the ions shows that the "empty-core" model [27] is the one which, despite its simplicity, better reproduces the thermodynamic and structural properties of liquid lithium in a wide range of temperatures. The empty-core model is explicitly adopted in the implementation of the PST potential; the only other model "competitive" with the empty-core one turns out to be the potential adopted in Refs. [10,15]. In any case, it must be reminded that an accurate determination of the spectral features near $\omega = 0$ either by INS or by MD techniques is not a trivial task; thus, the actual importance of the discrepancies should not be overvalued.

As is well known, the relevant information over the collective dynamics of density fluctuations over different length scales is provided by the intermediate scattering function $F(k,t)$ evaluated at different wave vectors. At all the three temperatures of interest, the quantity $F(k,t)$ as obtained in our simulations is found to exhibit an oscillatory behavior, which persists for all wave vectors $k \leq k_0 \approx 1.8$ Å^{-1}. These oscillations give rise to a well defined inelastic peak in $S(k,\omega)$ up to $k_0 \approx 0.75\ k_m$, where k_m denotes the position of the main peak of $S(k)$. This feature appears to be common to all the alkali metals in proximity of their respective melting points [14].

The MD results for the peak frequency $\omega_{peak}(k)$ are reported in Fig. 6, which refers to two different temperatures. Specifically, in Fig. 6(a) the simulation findings at 470 K are compared with the corresponding INS data, while in Fig. 6(b) the MD results at 526 K are compared with the IXS data by Burkel [7] at $T = 533$ K. Considering the difficulty to extract the relevant information from the INS experiment, and the still moderate accuracy of the IXS techniques, the overall agreement can be considered as satisfactory. In particular, the INS data reported in Fig. 6(a) have been deduced from the high-energy, low-resolution MARI experiment, assuming that $S_{tot}(k,\omega)$ can be written as a sum of three Lorentzians [representing the inelastic and quasielastic collective features embodied in $S(k,\omega)$], plus a Gaussian [which accounts for the resolution-broadened peak of the self-contribution $S_s(k,\omega)$].

A common feature in the dispersion relation of all liquid alkali metals at small wave vectors is the observation of an *increase* of the slope of $\omega_{peak}(k)$ with respect to the one implied by the hydrodynamic sound velocity [2,9,14,24]. In our MD data, this "positive dispersion" has been detected at all the three state points investigated, which a maximum increase of the effective sound velocity $\omega_{peak}(k)/k$ with respect to the hydrodynamic value, which ranges from 20 to 22%, depending on the considered temperature. The effect (known to be due to "shear relaxation" processes [28]) can be quantitatively accounted for by a viscoelastic theory [29], as verified in

the other molten alkali metals [9,15,30], in dense Lennard-Jones fluids [28] and in liquid water [30]. In the alkali metals, the same viscoelastic model is also found to account for the main features of the entire dispersion relation [30].

V. SINGLE-PARTICLE DYNAMICS

The above-mentioned success of a simple viscoelastic approach in reproducing the spectral features of $S(k,\omega)$ reflects the strong influence of structural effects on collective dynamics. In fact, the basic structural information is embodied in the second and fourth frequency moments, and these two quantities are correctly incorporated into the theoretical framework. Moreover, a typical assumption of all viscoelastic models is the characterization of the relaxation processes by a single microscopic decay time, which usually turns out to be very short [29,30]. As a consequence, even if long-lasting phenomena of the form discussed later on in this section may have some relevance on the low-frequency portion of $S(k,\omega)$, in practice the main features of the spectra (such as the position of the inelastic peaks, the occurrence of de Gennes narrowing, etc.) are in fact ruled by the leading structural (or mean-field) effects.

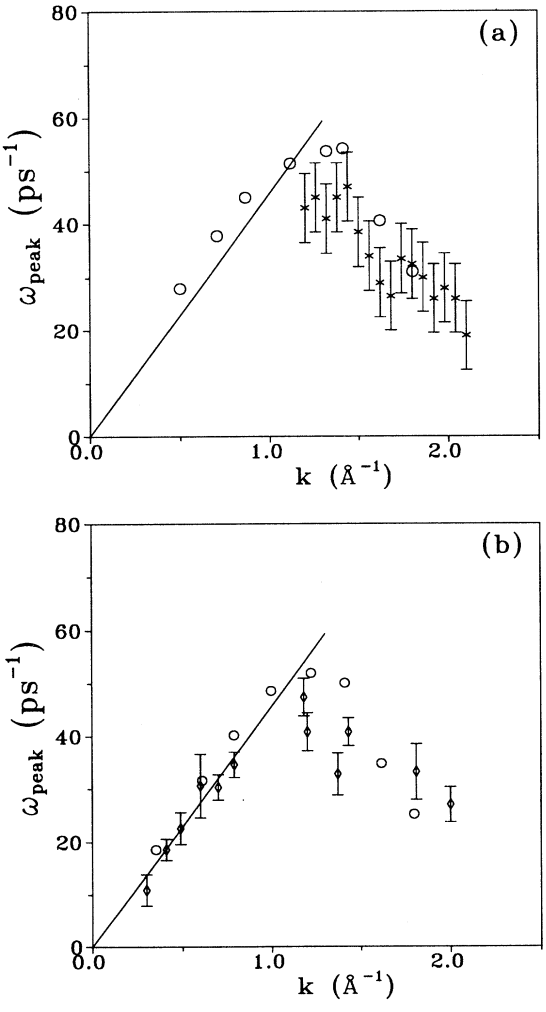

FIG. 6. Dispersion relation of the peak frequencies of $S(k,\omega)$ of liquid Li at the temperatures $T=470$ K (a) and $T=526$ K (b). Circles, our MD results: asterisks, neutron data at 470 K [5]: lozenges, IXS data at $T=533$ K [7].

In contrast, the relevance of slowly decaying relaxation channels appears to be much more marked in other cases where structural effects have an indirect (or negligible) weight. The Green-Kubo integrands for the transport coefficients, and the single-particle time correlation functions are typical examples of these quantities. To cope with such a situation, a theory more refined than one based on a single relaxation-time assumption is clearly needed.

In this work we shall limit our analysis of these more complicated cases to the normalized *velocity autocorrelation function* (VACF) $\Psi(t)$ and to the *self-intermediate scattering function* $F_s(k,t)$, along with the corresponding frequency spectrum $S_s(k,\omega)$. In particular, we shall focus our attention on two quantities.

(i) The VACF memory function $K(t)$, defined through the equation

$$\hat{\Psi}(z)=[z+\hat{K}(z)]^{-1}\ , \tag{2}$$

where $\hat{\Psi}(z)$ and $\hat{K}(z)$ are the Laplace transforms of the corresponding time correlations, and $z=i\omega+0^+$ is a complex variable.

(ii) The second-order memory function $M_s(k,t)$ of $F_s(k,t)$, which satisfies the equation

$$\hat{F}_s(k,z)=\left[z+\frac{(k_BT/m)k^2}{z+\hat{M}_s(k,z)}\right]^{-1}\ . \tag{3}$$

As is well known, in the hydrodynamic limit $k\to 0$ the memory function $M_s(k,t)$ coincides with $K(t)$. Another important relation connects $K(t)$ with the diffusion coefficient

$$D=(k_BT/m)\left[\int_0^\infty dt\,K(t)\right]^{-1}\ . \tag{4}$$

In dense fluids, the importance of dealing with memory functions is nowadays connected with the development in the last decade of several nonphenomenological approaches, which are explicitly phrased in terms of these dynamical quantities [19–21]. The basic result of these theories is that a general memory function $M(t)$ can be split into two contributions having a different physical origin

$$M(t)=M^{(B)}(t)+M^{(R)}(t)\ . \tag{5}$$

Here the first term (which is the dominant one at short times) stems from "binary collisions." In view of the fast character of these events, $M^{(B)}(t)$ decays rapidly to zero, and beyond a certain time the full memory function is entirely determined by the other contribution $M^{(R)}(t)$. Broadly speaking, the origin of this second term is due to long-lasting correlation effects among the collisions. Since these "recollision" effects require a finite time to

develop, initially $M^{(R)}(t)$ is almost negligible. However, at intermediate and long times the slowly decaying character of this term takes over, and gives rise to a "tail" of $M(t)$. The specific form of these slow contributions depends on the particular problem under consideration, but in principle can be determined by relatively simple "mode-coupling" concepts [20,31]. Even so, the practical use of this formalism is far from being straightforward; for instance, a rigorous application of the theoretical framework of Refs. [20,21] requires the self-consistent determination of several time correlation functions in an extended range of wave vectors, followed by rather heavy numerical calculations. In many cases of physical interest, it is fortunately possible to make a number of approximations which, besides simplifying considerably the problem, permit a better appreciation of the fundamental processes underlying the phenomenon [11–14]. The MD data provide an important benchmark for the validity of the overall approach, particularly in those cases (such as the VACF) where the relevant information is not easily provided by real experiments.

A. The velocity autocorrelation function

Let us firstly consider the VACF memory function $K(t)$. As shown in [11], a reasonable approximation for the binary term $K^{(B)}(t)$ can be obtained by noticing that its decay is fast enough to be characterized by a single time constant $\tau_B=[2K(0)/|\ddot{K}(0)|]^{1/2}$. (Here the dots indicate time derivatives.) Near the melting point, a suitable functional form for this decay turns out to be [11]

$$K^{(B)}(t)\approx\Omega_0^2\,\mathrm{sech}^2(t/\tau_B)\ , \tag{6}$$

where Ω_0 is the so-called Einstein frequency, and the quantity $K^{(B)}(0)=\Omega_0^2$ coincides with the initial value $K(0)$ of the full memory function. As shown in [11], both Ω_0^2 and τ_B can be expressed in terms of integrals involving the pair potential $v(r)$ and the pair distribution function $g(r)$ [or the static structure factor $S(k)$].

The simple approximation $K(t)\approx K^{(B)}(t)$ is found to be too naive to account for the overall time dependence of the full memory function. In fact, in addition to a fast initial decay, $K(t)$ exhibits a long-lasting tail, which cannot be reproduced by Eq. (6). According to the theory, the tail should stem from a nonlinear coupling of the velocity of the particle with the slow dynamical variables of the fluid. In the case of a liquid near the melting point, the density is high enough that the relevant slow dynamical events at intermediate and long times are those associated with the sluggishness of the structural relaxation processes. As a consequence, the most important decay channels involve the density fluctuations (both collective and single particle). The contribution of these "density modes" to the recollision term can be written as [20]

$$K^{(R)}(t)=\frac{k_BT}{6\pi^2nm}\int_0^\infty dq\,q^4\frac{[S(q)-1]^2}{S(q)}\times[F_s(q,t)-F_0(q,t)]\frac{F(q,t)}{S(q)}\ , \tag{7}$$

where $F_0(q,t)=\exp[-(k_BT/2m)k^2t^2]$ is the free-particle limit of the intermediate scattering functions F and F_s. Because $K^{(R)}(t)$ should account for the long-lasting tail of the memory function, an important contribution to the integral (7) comes from the density fluctuations with $q\approx k_m$, which are characterized by a marked de Gennes slowing down. Pursuing this argument, one arrives at the following simplified expression [11]:

$$K^{(R)}(t)\approx\frac{k_BT}{6\pi^2nm}Ak_m^4[F_s(k_m,t)-F_0(k_m,t)]\frac{F(k_m,t)}{S(k_m)}\ , \tag{8}$$

where A is a purely structural quantity given by the area under the main peak of $[S(q)-1]$. In practice, to evaluate $K^{(R)}(t)$ we need suitable approximations for the quantities F_s and F. For this purpose, the self-intermediate scattering function can be expressed by the so-called "Gaussian approximation" [28]

$$F_s(k,t)\approx\exp[-(1/6)k^2\delta r^2(t)]\ , \tag{9}$$

where $\delta r^2(t)$ is the mean square displacement of a particle in the liquid. Equation (9) is exact both for small and large wave vectors, and is found to work rather well even for $k\approx k_m$ [17]. As far as F is concerned, we may adopt a simplified viscoelastic model [11–14]. This approximation has the merit that all the involved parameters can be evaluated in terms of structural quantities, and turns out to give good results for wave vectors $k\approx k_m$ [30].

Summing up, from Eqs. (6) and (8) we may evaluate the full memory function $K(t)=K^{(B)}(t)+K^{(R)}(t)$, with structural quantities and the mean square displacement $\delta r^2(t)$ as the only input information. The situation is even better for the diffusion coefficient D, which can be calculated from Eq. (4) by means of a self-consistent approach [11], which does not require the detailed knowledge of $\delta r^2(t)$. The results obtained in such a way for D are remarkably good for many typical simple liquids. More recently, González *et al.* [15] have improved this self-consistent scheme, with the final result of obtaining at the same time $K(t)$, $\Psi(t)$, and $\delta r^2(t)$ (and obviously D). A common feature of these approaches is the assumption that the leading decay channels for the tail of $K(t)$ are those involving the de Gennes density modes with wave vectors $\approx k_m$. This simplification leads to results that improve considerably those of a purely binary theory with $K(t)\equiv K^{(B)}(t)$; in particular, the decay rate of the long-lasting tail is now correctly reproduced.

A more stringent test, however, shows that the previous representation is much too simplified to account for all the details of the time dependence of the tail of $K(t)$. This is particularly true at intermediate times, where the actual memory function shows bumps and wiggles, which are not reproduced by the simple approximation (8) (cf., Fig. 8 in the following). To ascertain which wave vectors are really relevant in the integral in Eq. (7), we analyze the "vertex" $W(q)=q^4[S(q)-1]^2/S(q)$. As is apparent from Fig. 7, $W(q)$ exhibits several peaks, with zeros at the points where $S(q)=1$. Since for increasing wave vectors $F_s\to F_0$, the dominant contribution to $K^{(R)}(t)$ comes

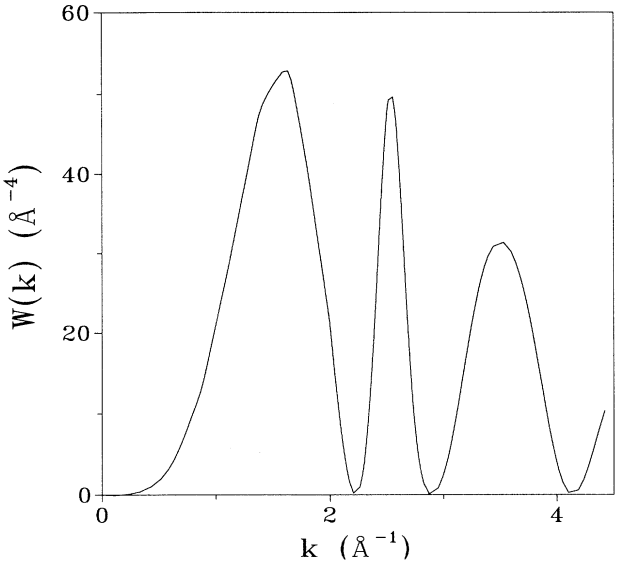

FIG. 7. The vertex $W(q)$ as evaluated in liquid lithium at 470 K.

in practice only from the first two peaks, located at $k_1 \approx 1.60$ Å^{-1} and at $k_2 \approx k_m$. Hence, for an accurate evaluation of $K^{(R)}(t)$ in addition to the de Gennes modes we need to include a second density mode with $q \approx k_1$. In this wave-vector range the intermediate scattering function $F(q,t)$ still exhibits an oscillatory behavior (cf., Sec. IV), which eventually gives rise to a "modulation effect" in the tail of $K(t)$.

Including the density modes at the wave vectors k_1, k_2 as the only relevant decay channels, the expression of $K^{(R)}(t)$ can be written as

$$K^{(R)}(t) \approx \frac{k_B T}{6\pi^2 n m} \sum_{i=1}^{2} W_i [F_s(k_i,t) - F_0(k_i,t)] \frac{F(k_i,t)}{S(k_i)} , \tag{10}$$

where W_i denotes the area under the ith peak of $W(q)$. This second approximation scheme improves the agreement with the MD data of $K(t)$ at intermediate times (Fig. 8); in particular, at $T=470$ K the theoretical memory function is found to nearly coincide at all times with the simulation results. The quality of the agreement instead is not so excellent at $T=574$ K, where in the time interval between 0.06 and 0.10 ps the theoretical results slightly overestimate the MD data. However, even in this case the wiggles and the tail of the memory function are well reproduced, indicating that the "mode-coupling" portion of $K(t)$ is indeed ruled by the density modes with wave vectors k_1 and k_2. As a consequence, the residual

TABLE III. Comparison among the results obtained for the diffusion coefficient (in units 10^{-5} cm^2/s) in liquid Li at the three state points considered in the present investigation. The theoretical values D have been deduced by integrating the memory function (4) within the approximations (8) and (10) for $K^{(R)}(t)$ (the results are denoted by 1 ch and 2 ch, respectively). The entries D_{MD} are the values found in our simulations. The experimental data D_{expt} refer either to direct measurements with a tracer technique[a] or to $k \to 0$ extrapolations of the neutron data obtained by two different INS experiments.[b,c]

Diffusion coefficient \ T (K)	470	526	574
D (1 ch)	6.82	8.34	9.66
D (2 ch)	7.21	8.99	10.52
D_{MD}	7.3±0.1	9.8±0.1	12.3±0.1
D_{expt}	6.7±0.6[a]	9.3±0.7[a]	11.6±0.9[a]
	6.4±0.4[b]	9.0±0.6[b]	10.8±0.3[b]
	6.9±0.9[c]	9.5±1.2[c]	11.9±1.4[c]

[a]See Ref. [33].
[b]See Ref. [5].
[c]See Ref. [6].

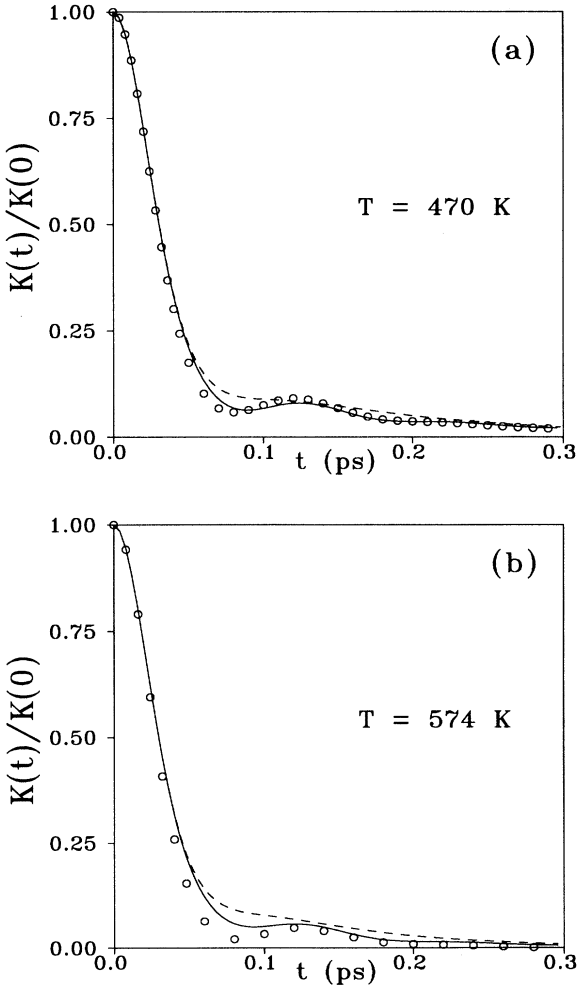

FIG. 8. The VACF memory function $K(t)$ at $T=470$ K (a) and 574 (b). The circles denote the simulation findings. The theoretical results obtained by taking for the recollision term the form (8) (dashed line) or (10) (full line) are also reported.

discrepancies at 574 K are likely to be due to our limited knowledge of the collisional part $K^{(B)}(t)$; in other words, although acceptable near the melting point, the ansatz (6) is likely to be oversimplified at increasing temperatures.

The diffusion coefficients predicted by the different approaches are compared in Table III with the actual values of D at the three different state points. Specifically, the MD values of D have been deduced from the slope of $\delta r^2(t)$, while the theoretical predictions follow from Eq. (4) by inserting for $K^{(R)}(t)$ either one of the approximations (8) and (10). It appears from Table III that the results of the improved scheme (10) compare rather well with the experimental and the MD values of D at the three temperatures. As it might be expected, the agreement is particularly good at 470 K; the larger discrepancies at 526 and 574 K are a clear consequence of the above-mentioned defects of the "binary" memory functions.

B. The self-spectrum at finite wave vectors

Let us finally consider the self-intermediate scattering function $F_s(k,t)$. At all wave vectors, the corresponding spectrum $S_s(k,\omega)$ is characterized by a monotonic decay from a peak value at $\omega=0$. Hence the k-dependent features of $S_s(k,\omega)$ can conveniently be summarized by considering the peak value $S_s(k,\omega=0)$ and the half-width at half maximum $\omega_{1/2}(k)$. It is customary to refer these quantities to the ones predicted by a diffusive model [namely $(\pi Dk^2)^{-1}$ and Dk^2, respectively] by introducing the dimensionless quantities $\Sigma(k)=\pi Dk^2 S_s(k,0)$ and $\Delta(k)=\omega_{1/2}(k)/Dk^2$. An alternative description makes use of the quantity $\omega_{1/2}(k)/k^2$, which can be interpreted as an effective k-dependent diffusion coefficient $D(k)$. Starting from the situation at $k=0$, where the diffusive model is exact and $\Sigma(0)=\Delta(0)=1$, we wish to investigate the wave-vector evolution of these quantities at the three temperatures of interest. In this paper, we shall limit our analysis to a limited range of "small" wave vectors ($0\le k\le 3.0$ Å^{-1}), which is particularly interesting from the theoretical point of view. A more extended description (which includes the k interval where one probes the details of collision processes) can be found in Ref. [32].

Our MD data for the quantity $D(k)=\Delta(k)D$ at the three state points are reported in Fig. 9(a). It appears that in all cases the diffusive limit is approached from below; moreover, $D(k)$ is found to exhibit a minimum at $k\approx k_m$. Since the size of the nearest neighbor shell is $\approx(2\pi/k_m)$, the presence of the minimum can be traced back to structural features (and, in particular, to the so-called "cage effect," which hinders somewhat the diffusive motion of the tagged particle). A similar trend is observed even in the simulation data at the high temperatures, and confirmed by the neutron findings of Ref. [5] [see Fig. 9(b) for the normalized half-width $\Delta(k)$]. These results in liquid lithium are fully consistent with the experimental data reported for another alkali metal, namely liquid sodium, in an extended range of temperatures [3,4].

In contrast, the MD data for $\Sigma(k)$ turn out to be more sensitive to changes in temperature. As illustrated in Fig. 10, the data show in fact a sort of "transition" in the temperature range from 526 to 574 K: while at 470 and 526 K $\Sigma(k)$ is a decreasing function of k, at 574 K this quantity is seen to *increase* with respect to its limiting value $\Sigma(0)=1$. Although this different behavior was not observed in the first measurements [3] in liquid Na [the results showed always an increasing $\Sigma(k)$, even near T_m], new more accurate data in the same liquid have detected a crossover analogous to the one in liquid Li [4]. By itself, the increase of $\Sigma(k)$ at the higher temperature may be attributed to a more pronounced relevance of the kinetic degrees of freedom (a free-particle model would

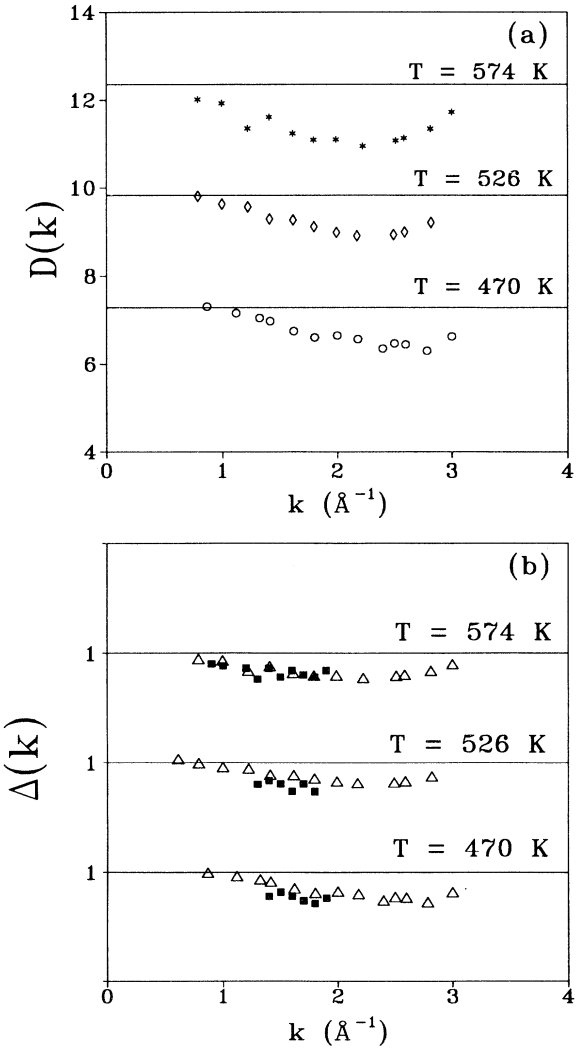

FIG. 9. (a) Wave-vector dependence of the MD data for the generalized diffusion coefficient $D(k)$. The data refer to $T=470$ (circles), 526 (lozenges), and 574 K (asterisks). (b) Comparison of the normalized half-widths $\Delta(k)$ at $T=470$, 526, and 574 K as found in the simulations (black squares) with those measured in the neutron experiments of Ref. [5] (open triangles).

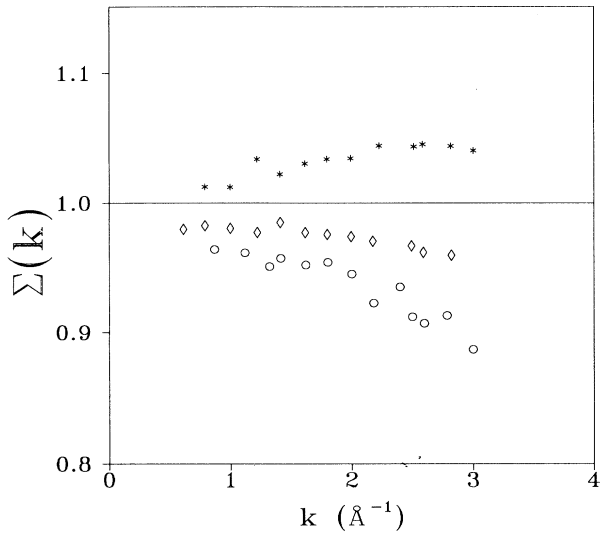

FIG. 10. Wave-vector dependence of the MD data for the normalized peak value $\Sigma(k)$.

indeed predict that $\Sigma(k) \propto k$). As the other alkali metals, lithium has a liquid phase that spans a rather wide temperature interval, ranging from a melting point at 453 K to a boiling point at 1620 K. Our MD data in liquid lithium seem to indicate that a rather modest temperature increase is sufficient to trigger the different behavior of $\Sigma(k)$. Even if this circumstance is probably true even in the other alkalis, a direct experimental evidence is still lacking. (The recent neutron measurements in liquid Na mentioned above [4] are limited to two state points, which are widely separated in temperature, $T=380$ K $\approx 1.02\ T_m$ and $T=900$ K.)

It is interesting to see whether all these pieces of "experimental" information can be interpreted in terms of a memory function framework analogous to the one discussed in the previous section for the VACF. For this purpose, the appropriate theoretical quantity is the second-order memory function $M_s(k,t)$ introduced in Eq. (3). Since $M_s(k\rightarrow 0,t)\rightarrow K(t)$, the approach is equivalent to a generalization of the previous framework at finite wave vectors. Even in the present case, the memory function can be split into a sum of "binary" and "recollision" terms namely, $M_s(k,t)=M_s^{(B)}(k,t)+M_s^{(R)}(k,t)$. Following Eq. (6), the binary contribution can be written as [14]

$$M_s^{(B)}(k,t)=[2(k_BT/m)k^2+\Omega_0^2]\mathrm{sech}^2[t/\tau_B(k)]\ , \qquad (11)$$

where we have tentatively adopted the same $\mathrm{sech}^2 x$ shape function used in the VACF case. In Eq. (11), the time $\tau_B(k)$ follows from [14]

$$\frac{1}{[\tau_B(k)]^2}=\frac{2\Omega_0^2/\tau_B^2+3(k_BT/m)k^2[2(k_BT/m)k^2+3\Omega_0^2]}{4(k_BT/m)k^2+2\Omega_0^2}\ . \qquad (12)$$

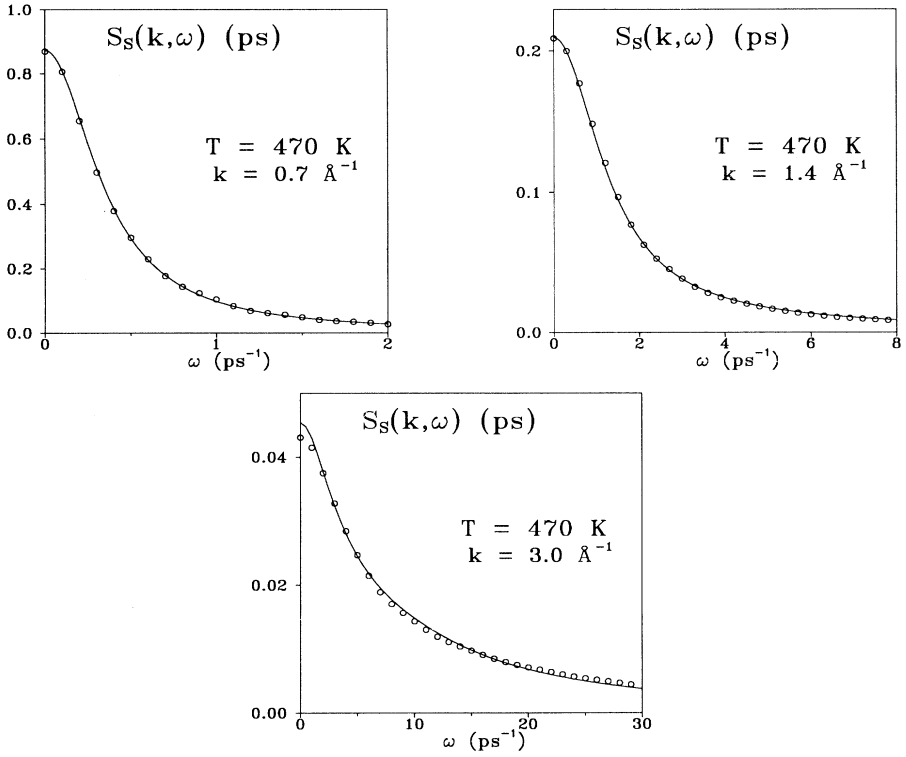

FIG. 11. The self-spectra $S_s(k,\omega)$ in liquid Li at 470 K. The circles denote our MD findings, the solid lines the corresponding theoretical predictions [obtained from Eq. (3) by adopting the approximation (14) for the memory function].

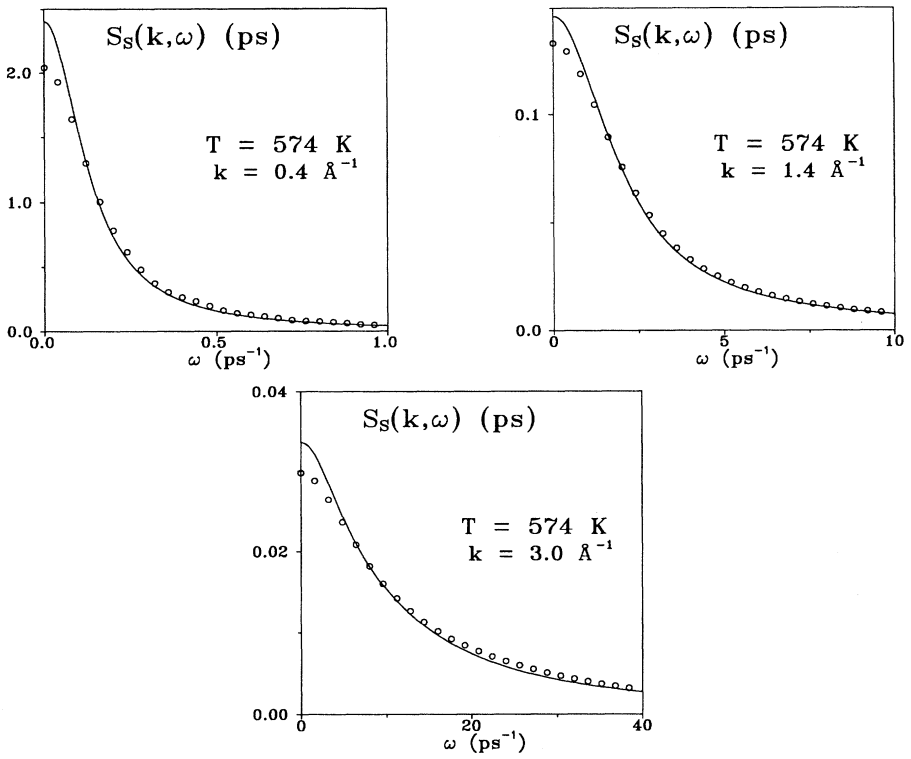

FIG. 12. As in the previous figure, but at a temperature $T=574$ K.

Clearly, $\tau_B(k\to 0)=\tau_B$. Equations (11) and (12) have the merit of describing at any k the correct decay of $M_s(k,t)$ at sufficiently short times. However, the MD data obtained in the other alkali metals [14,18,32] indicate that for $k\leq 2k_m$ the full memory function exhibits a tail, which cannot be accounted for only by $M_s^{(B)}(k,t)$. Consequently, even in this case we need to include a recollision term $M_s^{(R)}(k,t)$; considering as before only the contribution of density modes, this additional contribution can be written as [21]

$$M_s^{(R)}(k,t)=\frac{k_BT}{24\pi^3nm}\int d\mathbf{q}(q_z)^2\frac{[S(q)-1]^2}{S(q)} \times[F_s(|\mathbf{k}-\mathbf{q}|,t) -F_0(|\mathbf{k}-\mathbf{q}|,t)]\frac{F(q,t)}{S(q)}\ , \quad (13)$$

where the external wave vector $\mathbf{k}$ has been chosen along the z axis. Since the vertex appearing in (13) is similar to the one in Eq. (7), we may proceed to an approximate evaluation of $M_s^{(R)}(k,t)$ pursuing the same arguments adopted in the case of the VACF memory function. Specifically, in Eq. (13) we neglect all the density modes except those corresponding to $q\approx k_1$ and $q\approx k_2$. Performing the angular integrations, the simplified expression of the recollision term turns out to be

$$M_s^{(R)}(k,t)\approx\frac{k_BT}{2\pi^2nm}\sum_{i=1}^{2}W_i[\beta(k_i,t)-\beta_0(k_i,t)]\frac{F(k_i,t)}{S(k_i)}\ . \quad (14)$$

Here

$$\beta(k,t)=\exp[-\tfrac{1}{6}(k^2+k_m^2)\delta r^2(t)] \times\left[\left[\frac{1}{e(k,t)}+\frac{2}{e^3(k,t)}\right]\sinh[e(k,t)] -2\frac{\cosh[e(k,t)]}{e^2(k,t)}\right] \quad (15)$$

with

$$e(k,t)=\tfrac{1}{3}kk_i\delta r^2(t)\ . \quad (16)$$

In Eq. (14), the quantity $\beta_0(k,t)$ is defined by expressions similar to Eqs. (15) and (16), in which $\delta r^2(t)$ has been replaced by its free-particle counterpart $\delta r_0^2(t)=3(k_BT/m)t^2$. The details of the approximation (14) and the comparison with a single decay channel scheme are reported elsewhere [17,32].

Starting from the memory function $M_s(k,t)=M_s^{(B)}(k,t)+M_s^{(R)}(k,t)$, it is now possible to exploit Eq. (3) and evaluate the self-spectrum $S_s(k,\omega)=(1/\pi)\,\mathrm{Re}\hat{F}_s(k,z=i\omega+0^+)$. Figures 11 and 12 report at two temperatures the comparison of these theoretical results with the MD spectra. While the agreement is seen to be

quite good at 470 K, some deviations are apparent at 574 K in the low-frequency region. A consequence of these discrepancies is that in its present formulation the theory cannot account for the aforementioned increase of $\Sigma(k)$ with the wave vector as observed in the small k region at 574 K. The agreement is instead much better near the melting point, as illustrated by Fig. 13, which reports the theoretical predictions for $\Sigma(k)$ and $\Delta(k)$ at 470 K along with our MD data and the available neutron-scattering results [5].

The discrepancies apparent at 574 K parallel the ones noted previously at the same temperature for the VACF memory function. As in that case, they are likely to be due to the oversimplified form assumed for the binary contribution $M_s^{(B)}(k,t)$. Although Eq. (11) gives quite reasonable results near the melting point, its simple form appears to be inadequate at increasing temperatures. In principle, another possible source of discrepancy could be the onset of additional decay channels, different from those associated with the density modes. For instance, transverse current modes (the ones responsible for the formation of local vortex patterns) are certainly expected to become more important at increasing temperatures. The results obtained in the VACF case seem, however, to indicate that at the relatively low temperature of 574 K the relevance of these current modes is still rather small.

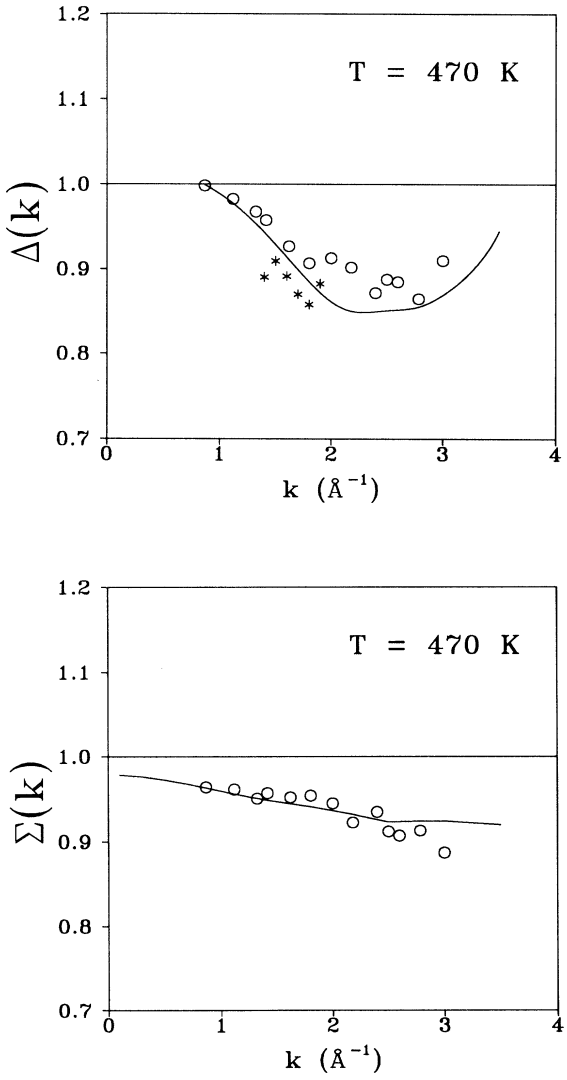

FIG. 13. The quantities $\Delta(k)$ and $\Sigma(k)$ in liquid Li at 470 K. The circles are our MD findings. The full lines denote the theoretical results [with the recollision term obtained by Eq. (14)]. The asterisks are the neutron-scattering results [5].

VI. CONCLUDING REMARKS

In the present paper we have investigated by computer simulation several structural and dynamical properties of liquid lithium at three different temperatures. The results have been compared with the data recently obtained by inelastic scattering of neutrons (and even of x-rays as far as collective motions are concerned). The overall quality of the agreement is good, supporting the idea that even in lithium we may adopt the same type of effective potential successfully tested in the heavier alkali metals. On the theoretical side, we have shown that a simplified mode-coupling approach is able to reproduce rather well several features of single-particle motion, including both the ordinary and the k-dependent diffusion coefficient. The agreement between the theoretical predictions and the data is particularly striking near the melting point, where the framework accounts for all the detailed features of the relevant memory functions. Some deviations become instead apparent at the highest temperature investigated. We are inclined to believe that the main source of these discrepancies lies in the simple form assumed for the binary memory function, which undoubtedly exhibits some flaws at increasing temperatures. Alternative, or additional, explanations (such as an increased role of the decay channels associated with the currents) are more unlikely, even if in principle they cannot be excluded. Work is in progress to fully clarify this point.

ACKNOWLEDGMENTS

We are indebted with Chr. Morkel and A. Stangl for fruitful discussions and for making available their experimental data before publication, and with D.J. González and K. Hoshino for the reports of their works. Our computer simulations were made possible by a convention between Consiglio Nazionale delle Richerche (CNR) and Centro Interuniversitario di Calcolo Elettronico dell'Italia Nord-Orientale (CINECA). P. de J. and P. V. acknowledge the financial support of the EEC Science Plan (Project No. SC1* CT91-0754).

[1] M. Shimoji, *Liquid Metals* (Academic, New York, 1977); N. H. March, *Liquid Metals* (Cambridge University Press, Cambridge, England, 1990).
[2] T. Bodensteiner, Chr. Morkel, P. Müller, and W. Gläser, J. Non-Cryst. Solids **117-8**, 941 (1990); Chr. Morkel and T. Bodensteiner, J. Phys. Condens. Matter **2**, SA251 (1990); T. Bodensteiner, Chr. Morkel, W. Gläser, and B. Dorner, Phys. Rev. A **45**, 5709 (1992).
[3] Chr. Morkel, C. Gronemeyer, W. Gläser, and J. Bosse, Phys. Rev. Lett. **18**, 1873 (1987); W. Montfrooy, I. de Schepper, J. Bosse, W. Gläser, and Chr. Morkel, Phys. Rev. A **33**, 1405 (1986).
[4] A. Stangl, Ph.D. thesis, Technische Universität Müchen, Germany, 1993.
[5] P. H. K. de Jong, P. Verkerk, S. Ahda, and L. A. van de Graaf, in *Recent Developments in the Physics of Fluids,* edited by W. S. Howells and A. K. Soper (Hilger, London, 1992); P. Verkerk, P. H. K. de Jong, M. Arai, S. M. Bennington, W. S. Howells, and A. D. Taylor, Physica B **180-181**, 834 (1992); P. H. K. de Jong, P. Verker, and L. A. de Graaf, J. Non-Cryst. Solids **156-8**, 48 (1993); P. H. K. de Jong, Ph.D. thesis, Technische Universiteit Delft, Netherlands, 1993.
[6] J. Sedlmeier, Ph.D. thesis, Technische Universität München, Germany, 1992.
[7] E. Burkel, *Inelastic Scattering of X-rays with very high Energy Resolution* (Springer-Verlag, Berlin, 1991).
[8] N. Matsuda, K. Hoshino and M. Watabe, J. Chem. Phys. **93**, 7350 (1990); N. Matsuda, H. Mori, K. Hoshino, and M. Watabe, J. Phys. Condens. Matter **3**, 827 (1991); K. Hoshino, H. Ugawa, and M. Watabe, J. Phys. Soc. Jpn. **61**, 2182 (1992); F. Shimojo, K. Hoshino, and M. Watabe, *ibid.* **63**, 141 (1994).
[9] S. Kambayashi and G. Kahl, Europhys. Lett. **18**, 421 (1992); Phys. Rev. A **46**, 3255 (1992).
[10] M. Canales, J. A. Padró, L. E. González, and M. Giró, J. Phys. Condens. Matter **5**, 3095 (1993).
[11] U. Balucani, R. Vallauri, T. Gaskell, and S. F. Duffy, J. Phys. Condens. Matter **2**, 5015 (1990); U. Balucani, S. F. Duffy, and R. Vallauri, in *Recent Developments in the Physics of Fluids* (Institute of Physics, Bristol, 1992), Sec. 2, F. 151.
[12] U. Balucani and R. Vallauri, Phys. Rev. A **40**, 2796 (1989).
[13] U. Balucani, Mol. Phys. **71**, 123 (1990).
[14] U. Balucani, A. Torcini, and R. Vallauri, Phys. Rev. A **46**, 2159 (1992); Phys. Rev. B **47**, 3011 (1993); J. Non-Cryst. Solids **156-158**, 43 (1993).
[15] L. E. González, D. J. González, M. Silbert, and J. A. Alonso, J. Phys. Condens. Matter **5**, 4283 (1993); L. E. González, D. J. González, and K. Hoshino, J. Phys. Condens. Matter **6**, 3849 (1994); L. E. González, D. J. González, and M. Canales (private communication).
[16] S. Ranganathan, K. N. Pathak, and Y. P. Varshni, Phys. Rev. E **49**, 2835 (1994); S. Ranganathan and K. N. Pathak, J. Phys. Condens. Matter **6**, 1309 (1994).
[17] A. Torcini, Ph.D. thesis, Università di Firenze, Italy 1994.
[18] W. van der Lugt and B. P. Alblas, in *Handbook of Thermodynamic and Transport Properties of Alkali Metals,* edited by R. W. Ohse (Blackwell, Oxford, 1985), p. 299.
[19] For a review, see, A. Sjölander, in *Amorphous and Liquid Materials,* edited by E. Lüscher, G. Fritsch, and G. Jacucci (Martinus Nijhoff, Dordrecht, 1987), p. 239.
[20] L. Sjögren and A. Sjölander, J. Phys. C **12**, 4369 (1979); L. Sjögren, *ibid.* **13**, 705 (1980); Phys. Rev. A **22**, 2866 (1980).
[21] G. Wahnström and L. Sjögren, J. Phys. C **15**, 401 (1982).
[22] P. G. de Gennes, Physica **25**, 825 (1959).
[23] D. L. Price, K. S. Singwi, and M. P. Tosi, Phys. Rev. B **2**, 2983 (1970).
[24] A. Rahman, Phys. Rev. A **9**, 1667 (1974).
[25] R. D. Mountain, in *Proceedings of the Third International Conference on Liquid Metals,* edited by R. Evans and D. A. Greenwood, IOP Conf. Proc. No. 30 (Institute of Physics and Physical Society, London, 1977), p. 62.
[26] K. Hornung, in *Handbook of Thermodynamic and Transport Properties of Alkali Metals* (Ref. 18), p. 487.
[27] N. W. Ashcroft, Phys. Lett. **23**, 48 (1966).
[28] J. P. Boon and S. Yip, *Molecular Hydrodynamics* (McGraw-Hill, New York, 1980).
[29] S. W. Lovesey, J. Phys. C **6**, 1856 (1973).
[30] U. Balucani, G. Ruocco, A. Torcini, and R. Vallauri, Phys. Rev. E **47**, 1677 (1993).
[31] See, e.g., U. Balucani, in *Molecular Liquids: New Perspectives in Physics and Chemistry,* edited by J. Teixeira-Dias (Kluwer, Dordrecht, 1992).
[32] U. Balucani, A. Torcini, A. Stangl, and Chr. Morkel, Phys. Scr. (to be published).
[33] L. Löwenberg and A. Lodding, Z. Naturforsch. Teil A **22**, 2077 (1967).